

Special  
Collection

# Spectroelectrochemical Properties of 1,10-Phenanthroline Substituted by Phenothiazine and Carbazole Redox-active Units

Jakub Wantulok,<sup>[a]</sup> Romana Sokolova,<sup>\*,[b]</sup> Ilaria Degano,<sup>[c]</sup> Viliam Kolivoska,<sup>[b]</sup> Jacek E. Nycz,<sup>[a]</sup> and Jan Fiedler<sup>[b]</sup>

*In memory to Prof. Jean-Michel Savéant, a founder of molecular electrochemistry, who we really miss dearly.*

Complexes of 1,10-phenanthrolines with cations of transition metals have broad range of applications. This work aims at designing and investigating phenothiazine and carbazole substituted 1,10-phenanthrolines as ligands for future complexes with transient metal cations. The combined electrochemical, spectroelectrochemical and DFT studies were employed to demonstrate the effect of broken symmetry in substituted 4,7-di(phenothiazine)-1,10-phenanthrolines on their

spectroelectrochemical properties. A reversible color change (new absorption band around 500 nm) due to phenothiazine radical cation was observed in the first oxidation step. Results further indicate that phenothiazine substituents behave as two equivalent but almost electronically isolated redox centres. The work additionally presents a comprehensive reaction mechanistic study of oxidation and reduction processes complemented by HPLC-MS/MS identification.

## 1. Introduction

The development of functional electrochemical compounds requires the fundamental understanding the relationship between their charge transfer properties and their chemical structure.<sup>[1]</sup> Optical changes of molecules upon the electron transfer reflect their electronic structure, which may be employed in their fundamental characterization. The tuning of absorption and electrochemical properties of organic compounds may be achieved by introducing or modifying substituents in their structure.<sup>[2]</sup> Here, new compounds based on 1,10-phenanthroline functionalized by phenothiazine and carbazole units (compounds **1** to **4**, Scheme 1) as possible ligands for further complexation with metal cations are described. Among other applications, phenanthrolines are of

great interest due to metal chelation<sup>[3]</sup> and have already been successfully implemented as functional optical units either in organic polymeric films or coordinated on transition metals in polymers.<sup>[4]</sup> Carbazole and phenothiazine are three-ringed aromatic secondary amines, whose electrochemical behaviour has already been described in detail.<sup>[5]</sup> In particular, as they contain a nitrogen heteroatom in their chemical structure, their oxidation and reduction lead to the formation of radical cation and anion, respectively, which is followed by subsequent redox process or a chemical reaction according to the chemical environment.<sup>[6]</sup> Carbazole and phenothiazine belong to electron-donor substituents. The main structural feature of phenothiazine is the presence of sulphur atom leading to a characteristic change of planarity of the two phenothiazine benzene rings. Carbazole derivatives have been widely employed as active components of organic light-emitting diodes<sup>[7]</sup> or organic photovoltaic cells.<sup>[8]</sup> Carbazole was further identified as an efficient and attractive redox active sensitizer in dye-sensitized solar cells thanks to its electrochemical and optical properties and thermal stability.<sup>[9]</sup> Phenothiazines were also investigated as possible organic redox polymeric materials.<sup>[10]</sup>

Additionally, due to diverse biological activity of carbazole and phenothiazine substituents, the proposed novel molecules are expected to exhibit bioactive properties. In many cases, their mechanism of action has not been fully understood. Carbazole and phenothiazine units are present in natural products, as well as in pharmaceuticals and in many bioactive species.<sup>[11]</sup> Modifying the phenothiazine structure in N-position by other N-heterocyclic fragments such as 1,10-phenanthroline units may benefit not only from their perspective biological properties.<sup>[12]</sup> The N-Arylated phenothiazine derivatives have anti-cancer, anti-bacterial, anti-fungal, anti-inflammatory and anti-oxidant activity, suppressing the drug resistance and bacterial redox activity and in vitro significant antioxidant

[a] J. Wantulok, J. E. Nycz  
Institute of Chemistry  
University of Silesia in Katowice  
ul. Szkolna 9; 40-007 Katowice, Poland

[b] R. Sokolova, V. Kolivoska, J. Fiedler  
Department Electrochemistry at the Nanoscale  
J. Heyrovský Institute of Physical Chemistry of the Czech Academy of Sciences  
Dolejšková 3, 18223 Prague, Czech Republic  
E-mail: sokolova@jh-inst.cas.cz

[c] I. Degano  
Department of Chemistry and Industrial Chemistry  
University of Pisa  
Via Moruzzi 13, 56124 Pisa, Italy



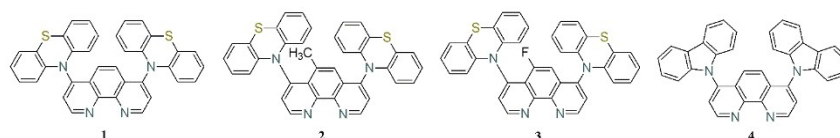
Supporting information for this article is available on the WWW under <https://doi.org/10.1002/celc.202100835>



An invited contribution to a joint Special Collection in memory of Prof. Jean-Michel Savéant



© 2021 The Authors. ChemElectroChem published by Wiley-VCH GmbH. This is an open access article under the terms of the Creative Commons Attribution License, which permits use, distribution and reproduction in any medium, provided the original work is properly cited.



**Scheme 1.** Chemical structure of 4,7-di(phenothiazine)-1,10-phenanthroline **1**, 5-methyl-4,7-di(phenothiazine)-1,10-phenanthroline **2**, 5-fluoro-4,7-di(phenothiazine)-1,10-phenanthroline **3** and 4,7-di(carbazole)-1,10-phenanthroline **4**.

**Table 1.** Peak potential values of compounds **1–4** for oxidation ( $E_p^{I-III}$ ) and reduction ( $E_p^{1-5}$ ) recorded in acetonitrile and 0.1 M TBAPF<sub>6</sub> against Ag|AgCl|1 M LiCl and energies of frontier orbitals (HOMO, HOMO(−1) and LUMO) calculated by DFT referenced against vacuum.

	$E_{\text{HOMO}}/\text{eV}$	$E_{\text{HOMO}(-1)}/\text{eV}$	$E_p^I/\text{V}$	$E_p^{II}/E_p^{II'}/\text{V}$	$E_p^{III}/\text{V}$	$E_{\text{LUMO}}/\text{eV}$	$E_p^1/\text{V}$	$E_p^2/\text{V}$	$E_p^3/\text{V}$	$E_p^4/\text{V}$	$E_p^5/\text{V}$
<b>1</b>	−5.2	−5.2	1.12	1.70 1.78	1.89	−1.76	−1.08	−1.54	−1.63	−1.78	−2.00
<b>2</b>	−5.1	−5.2	1.09	1.67 1.75	1.84	−1.75	−1.07	−1.55	−1.66	−1.77	−2.03
<b>3</b>	−5.0	−5.3	1.05	1.63 1.71	1.81	−1.95	−1.11	−1.51	−1.63	−1.77	−2.00
<b>4</b>	−5.6	−5.6	1.78	–	1.88	−1.80	−1.10	−1.54	−1.67	−1.78	−2.03

properties.<sup>[12a,13]</sup> It was further shown that these derivatives may be used as initiators in atom transfer radical polymerization<sup>[14]</sup> or emitter substances in organic light-emitting diodes.<sup>[15]</sup>

In this work, inspired by our recent findings in the reduction and oxidation mechanisms of *N*-pyrrolidinyl derivatives of 1,10-phenanthrolines,<sup>[16]</sup> we present an innovative idea of substituting 1,10-phenanthroline by phenothiazine and carbazole (compounds **1** to **4**, see Scheme 1) redox active moieties to create novel ligands for future complexes with transition metal complexes with specific redox and optical properties. Comprehensive electrochemical and spectroelectrochemical analysis of these derivatives is carried out. The chemical structure of phenothiazine derivatives systematically varied by the substitution of CH<sub>3</sub> or F in position 5 of 1,10-phenanthroline was explored (compounds **2** and **3**), to evaluate the effects of a geometrical asymmetry as well as inductive effects on their behaviour. Electrochemical characterization of these derivatives is complemented by the identification of intermediates and products of the electron transfer processes employing *in-situ* UV-Vis and IR spectroelectrochemical as well analytical separation/detection tools. Such designed combined investigation aims at elucidating reaction mechanisms of redox processes with the prospect of designing novel complexes.

## 2. Results and Discussion

### 2.1. Electrochemistry

#### 2.1.1. Oxidation of Compounds 1–3

The electrochemical oxidation of compounds **1** to **4** was investigated in acetonitrile by cyclic voltammetry combined with DFT calculations. The potential of the oxidation peaks and the values of HOMO energies referenced against vacuum are summarized in Table 1. The symmetric molecule **1** exhibits four

oxidation peaks, labelled I, II, II' and III (Figure 1A) with peak potentials 1.12, 1.70, 1.78 and 1.89 V, respectively. Linear dependence of the Faradaic peak currents on the square root of scan rate (Figure S1) proves the diffusion-controlled character of redox processes. Controlled potential coulometry performed at the potential slightly positive to the first oxidation peak (1.2 V vs. Ag|AgCl|1 M LiCl reference electrode) confirmed the consumption of two electrons per molecule in this process. The peak potential of the first oxidation process (1.12 V) does not change with neither increasing scan rate nor concentration of

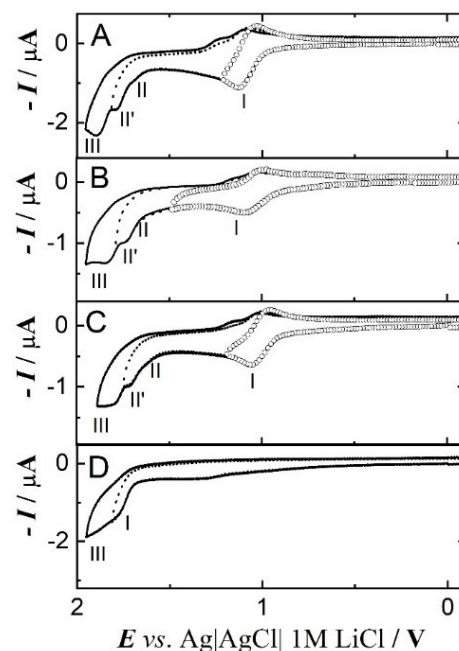


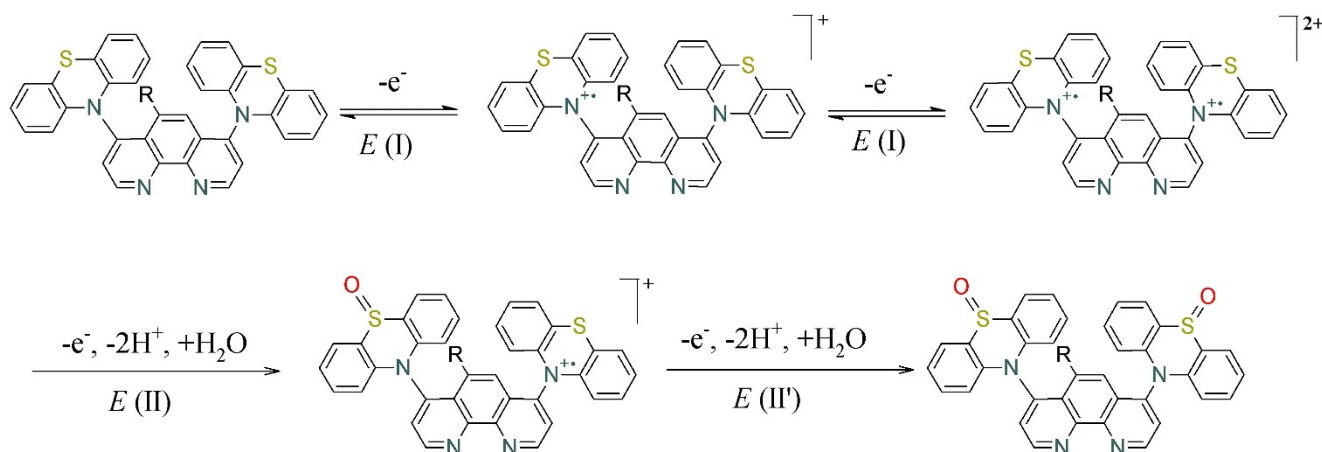
**Figure 1.** Cyclic voltammograms of A) 0.20 mM **1**, B) 0.13 mM **2**, C) 0.15 mM **3** and D) 0.30 mM **4** in CH<sub>3</sub>CN/0.1 M TBAPF<sub>6</sub> on glassy carbon electrode. The scan rate was 0.1 V · s<sup>−1</sup>.

compound **1** (Figure S2), as expected for a reversible transfer of electron(s). On the contrary, the experimentally observed peak-to-peak separation  $|E_p^a - E_p^c| = 88$  mV (see Figure 1A, empty circles) deviates from the value expected for a reversible two-electron step (29.5 mV), implying that the observed pair of maxima is due to overlapped two one-electron processes at close standard redox potentials. Furthermore, the peak current corresponds rather to twofold value in comparison to a one-electron process (ferrocene used for this comparison) and not to  $2^{3/2}$  ( $\sim 2.8$ ) times higher value expected for the simultaneous transfer of two electrons (see Randles-Sevcik equation).<sup>[17]</sup> Furthermore, convolution voltammetry (semi-integration of linear sweep voltammograms) was used to obtain data in the format suitable for further analysis according to literature<sup>[18]</sup> (see also Experimental part). The semi-integration of anodic current and subsequent logarithmic analysis results in the  $RT/nF$  slope of 105 mV (where symbols bear their standard meaning), which according to the established procedure (explained in detail in reference<sup>[17]</sup>) corresponds to two one-electron processes with their standard redox potential values spaced by 62 mV. In the case of independent, electronically non-communicating centres the electron transfer from the first and second centre proceeds at approximately equal potential ( $\Delta E^\circ = (RT/nF) \ln 4$ , i.e. 35.6 mV at 298 °C<sup>[19]</sup>) resulting in one-electron-like (by shape) wave in the voltammetry. When the centres electronically communicate, the voltammetric waves can be more separated.

The results lead us to conclude that the  $1 + 1e^-$  oxidation processes occur on two almost independent phenothiazine redox centres attached to the 1,10-phenanthroline moiety in equivalent (4 and 7) positions (see Scheme 2). This finding is further corroborated by theoretical (DFT) calculations. They clearly demonstrate that the degenerated HOMO and HOMO ( $-1$ ) are localized on phenothiazine substituents (Figure S3) and have energies  $E_{\text{HOMO}}(\mathbf{1}) = E_{\text{HOMO}(-1)}(\mathbf{1}) = -5.2$  eV, respectively. Further oxidation of phenothiazine substituents to their

sulfoxide proceeds at 1.70 V (wave II) and 1.78 V (wave II') (Scheme 2). The oxidation wave III at 1.89 V is attributed to the oxidation of 1,10-phenanthroline moiety (the oxidation of unsubstituted 1,10-phenanthroline has the peak potential at 1.90 V).<sup>[16]</sup>

The first oxidation process of **2** and **3** occurs at 1.09 and 1.05 V, respectively (Figure 1B,C). Both values are slightly negatively shifted compared to the oxidation potential of **1**. Such shifts, being in the same direction for both **2** and **3**, cannot be ascribed to an electron withdrawing or electron donating effect of fluorine and methyl substituents on the 1,10-phenanthroline core, respectively. This confirms that the electronic communication between the 1,10-phenanthroline moiety and phenothiazine redox centres is very limited. Similarly, as observed for **1**, the analysis of the cyclic voltammograms revealed only little higher anodic-to-cathodic peak-to-peak separations ( $|E_p^a - E_p^c| = 87$  mV and 82 mV for **2** and **3** respectively) than the theoretical prediction (see the discussion above). Importantly, the reversibility of the first charge transfer process is retained upon introducing methyl and fluorine substituents (see empty circles in Figure 1B,C). The peak potentials do not vary with neither scan rate nor the compound concentration. Albeit the compounds **2** and **3** both lack the symmetry and DFT shows slightly energetically separated HOMO and HOMO( $-1$ ) orbitals (see Table 1), the oxidation mechanism appears to be the same as for the compound **1**. The oxidation of both phenothiazines is terminated in the irreversible waves II and II' at 1.67 and 1.75 V for **2** and 1.63 and 1.71 V for **3** (Figure 1) ultimately leading to sulfoxide derivatives (Scheme 2). HPLC-MS/MS allowed the identification of the sulfoxide (two isomers) and the di(sulfoxide) (see below, part Identification of products). Oxidation of 1,10-phenanthroline core occurs at the wave III.<sup>[16]</sup>



R = H (**1**), CH<sub>3</sub> (**2**), F (**3**)

Scheme 2. Oxidation mechanism of compounds **1**, **2** and **3**.

### 2.1.2. Oxidation of Compound 4

The cyclic voltammetry of compound 4 shows two overlapping irreversible oxidation waves at 1.78 ( $E^I$ ) and 1.88 V ( $E^{II}$ ) (Figure 1D, Table 1). The linear relationship between the Faradaic peak current and square root of scan rate (Figure S1D) proves the diffusion-controlled character of the redox process. In the contrary to compounds 1–3, the peak potential scales linearly with the scan rate and concentration, being the slope  $\delta E_p/\delta \log v = 17$  mV and  $\delta E_p/\delta \log c = 18$  mV (Figure S4). This result approaches theoretical values 19 mV/decade for EC<sup>2</sup> reaction scheme<sup>[20]</sup> implying that after the removal of first electron the formed radical cation undergoes a chemical reaction, most probably dimerization (see below). The formation of a dimer in the case of organic amines and carbazole derivatives was described in literature<sup>[6a,21]</sup> and the spectroelectrochemical investigation performed in this work supports this hypothesis (see below).

### 2.1.3. Reduction of Compounds 1–4

Reduction properties of the compounds with fused aromatic rings are substantially determined by low lying  $\pi$ -orbital system of the rings. This system can be strongly influenced when a coordination to metals is established. Therefore, the reduction properties of compounds 1–4 designed as ligands for complexes and chromophoric materials are documented here, however investigated in less details than the oxidation properties of these substances. The cyclic voltammograms obtained for the reduction of compounds 1–4 (Figure 2) show five cathodic waves corresponding to the reduction of 1,10-phenanthroline moiety in the molecules. Reduction of 1,10-phenanthroline in solution of 0.1 M TBAPF<sub>6</sub> in acetonitrile is shown in recent article.<sup>[16]</sup> The spatial distribution of LUMO is shown in Figure S3. The values of LUMO energies referenced against vacuum correlate to the obtained cathodic peak potentials and are summarized in Table 1. All five reduction waves are irreversible. The first of them was investigated in larger detail. It is diffusion controlled as confirmed by linear dependence of the Faradaic peak current on the square root of the scan rate (see Figure S9). The dependences of the peak potential on the scan rate and compound concentration suggest an ECE mechanism (results  $\delta E_p/\delta \log v = 24$  and 29 mV and  $\delta E_p/\delta \log c = 33$  and 30 mV for 1 and 2, and  $\delta E_p/\delta \log v = 32$  and 29 mV and  $\delta E_p/\delta \log c = 33$  and 26 mV for 3 and 4, respectively, Figure S8).

### 2.2. UV-Vis Spectroelectrochemistry

The absorption spectrum of 1 exhibits bands at 203, 239, 253, 269 and 325 nm (Figure 3A, blue curve). During oxidation, new absorption bands at 210, 232, 265, 275 and 510 nm of  $1^{2+}$  (red curve) appear. The change of the absorption spectra during backward reduction of electrogenerated  $1^{2+}$  confirms that the redox process is chemically reversible (Figure 3B). The new

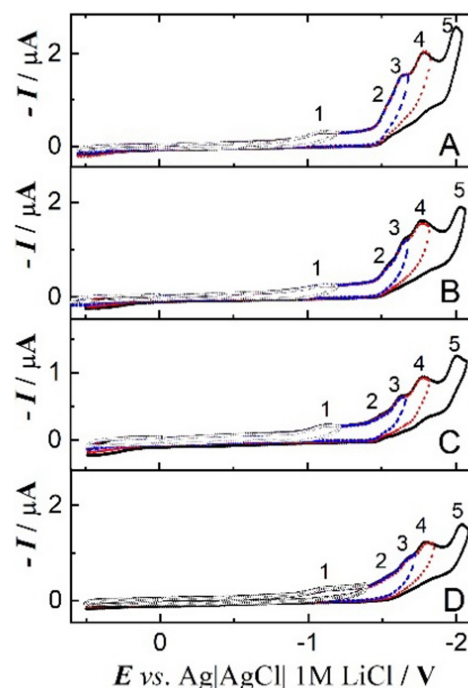


**Figure 2.** Cyclic voltammograms of A) 0.20 mM 1, B) 0.18 mM 2, C) 0.15 mM 3 and D) 0.30 mM 4 in CH<sub>3</sub>CN/0.1 M TBAPF<sub>6</sub> on glassy carbon electrode. The scan rate was 0.1 V·s<sup>-1</sup>.

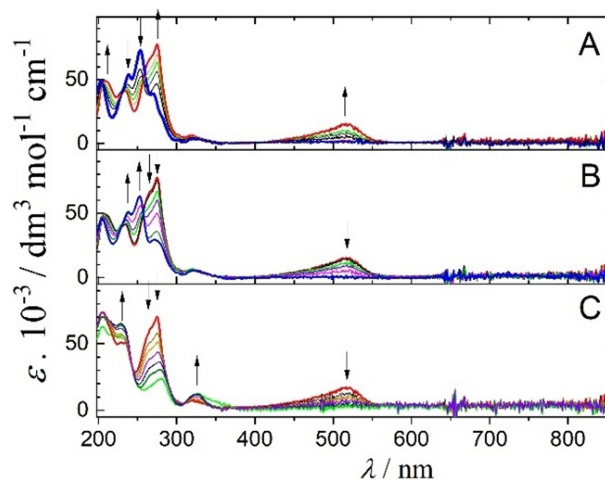


**Figure 3.** UV-Vis spectroelectrochemistry of 1 during A) oxidation  $1 \rightarrow 1^{2+}$  (first oxidation process I, spectra registered at potentials 0.50, 0.80, 0.95, 1.00, 1.15 and 1.20 V), B) rereduction (backward reduction of generated intermediate  $1^{2+} \rightarrow 1$ ) and C) further oxidation  $1^{2+} \rightarrow 1$  di(sulfoxide) (second oxidation process at II + II', spectra registered at potentials 1.20, 1.30, 1.40, 1.50, 1.60, 1.70 and 1.80 V).

band in the visible region (at 510 nm, resulting into greenish color) obviously originates from the formation of a singly occupied orbital (SOMO) on the oxidized phenothiazine units of  $1^{2+}$ . Consequently, when applying the potential corresponding to the second oxidation step II + II', the band at 510 nm and greenish colour disappears (Figure 3C).

The spectral changes during the oxidation of 2 and 3 are in the UV and visible region are similar as observed for 1 (see

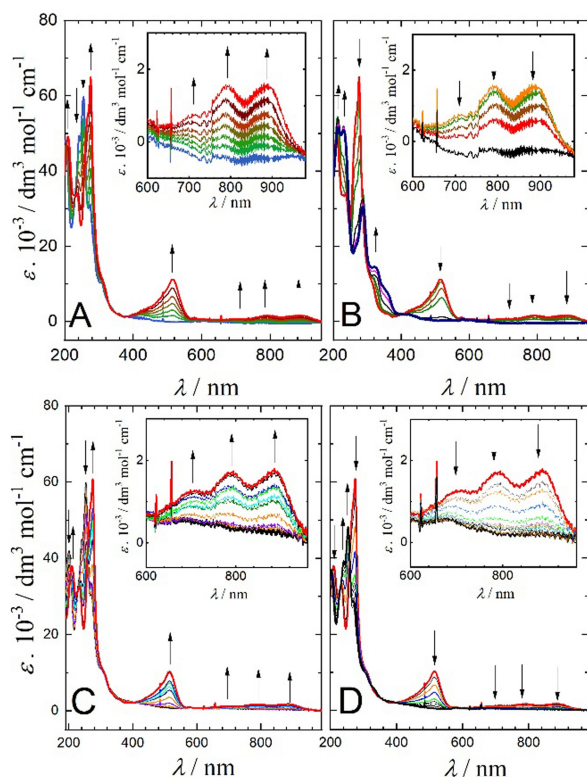


Table 2). In addition, low intense bands were detected at longer wavelengths (at 705, 790 and 886 nm) for both  $2^{2+}$  and  $3^{2+}$  (Figure 4 C, D). These bands (as well as the band peaking at 514 nm) are associated with the presence of SOMO on the half-

**Table 2.** Values of absorption maxima and molar extinction coefficients obtained for 1–4 and their dications.

compound	$\lambda_{\text{max}}/\text{nm}$ ( $\epsilon/10^3 \text{ M}^{-1}\text{cm}^{-1}$ , sh: shoulder)			
	1	2	3	4
1–4	203 (49.1) 239 (54.1) 253 (73.1) 269 (38.9) 325 (3.7)	202 (47.5) 241 (49.2) 254 (59.6) 274 (30.5) 306sh (10.4)	200 (41.8) 240 (44.6) 253 (59.6) 269 (31.0) 306 (9.9)	210 (30.4) 231 (60.4) 270 (22.2) 275 (22.0) 319 (6.1) 331 (6.3)
dication 1–4 $^{2+}$	210 (49.1) 232 (41.2) 265sh (66.8) 275 (77.3) 321 (6.2) 514 (16.5)	210 (49.3) 236 (33.8) 267sh (55.3) 275 (64.5) 428 (3.1) 514 (10.9) 705 (0.7) 790 (1.5) 886 (1.5)	210 (37.8) 231 (32.1) 268sh (53.9) 274 (60.6) 306 (9.9) 488sh (6.4) 514 (10.2) 705 (1.2) 790 (1.7) 886 (1.7)	210 (49.7) 231 (86.9) 277 (36.0) 313 (8.7) 328 (7.8) 388 (6.1)

\* In the case of 4 the spectrum belongs to a mixture of products (see Scheme 3).



**Figure 4.** UV-Vis spectroelectrochemistry of 2 during A) oxidation  $2 \rightarrow 2^{2+}$  (first oxidation process I, spectra registered at potentials 0.50, 0.80, 0.95, 1.00, 1.15, 1.20 and 1.25 V), B) oxidation  $2^{2+} \rightarrow 2\text{-di(sulfoxide)}$  (second oxidation process at II + II', spectra registered at potentials 1.25, 1.40, 1.50, 1.60 and 1.75 V). UV-Vis spectroelectrochemistry of 3 during C) oxidation  $3 \rightarrow 3^{2+}$  (first oxidation process I, spectra registered at potentials 0.50, 0.65, 0.70, 0.75, 0.80, 0.85, 0.90, 0.95, 1.00 and 1.15 V) and D) rereduction (backward reduction of generated intermediate  $3^{2+} \rightarrow 3$ ).

oxidized phenothiazine units and disappear in the second oxidation step. In comparison to compound 1, which does not exhibit spectroelectrochemically detectable bands above 600 nm (Figure 3), the increased intensity and therefore detectable long wavelength bands with 2 and 3 are attributed to the lower symmetry of these (methyl- or fluoro- substituted) compounds.

The absorption maxima and extinction coefficients of all studied compounds and their dications are summarized in Table 2. Transients of absorption spectra of the newly developed band at 514 nm at the first oxidation step of compounds 1 to 3 and their subsequent reduction (Figure 5) confirms the reversibility of this electron transfer process.

The absorption spectrum of 4 (Figure 6, black curve) with characteristic bands at 231, 275 and 331 nm during oxidation results in the increase of absorption bands at 210, 231, 277 and 388 nm (Figure 6, red curve, Table 2). The spectral changes are attributed to the formation of a radical cation and biradical dication (one or two carbazole substituents oxidized) as intermediates and of the final dimeric products (see Scheme 3). When applying potential values higher than 1.8 V (i.e. beyond the peak I, see Figure 1D), the spectral response changes, the band at 338 nm shifts bathochromically to 410 nm and a new band at 720 nm appears (dotted and dashed curves in Figure 6). During the rereduction (performed at  $-0.2$  V, Figure S5) the bands at 410 and 720 nm disappear, and the final spectrum is similar to the original spectrum of 4; however, the intensities of the original bands are different. As electrochemical and spectroscopic results show, the compound 4 does not show repeatable switching due to the presence of a chemical reaction.

### 2.3. NIR Spectroelectrochemistry

An attempt was performed to detect “organic” inter-valence charge transfer (IVCT) bands which could be expected in the NIR region in the case of electronic interaction between two equivalent oxidation centres on phenazine or carbazole units. Such bands would increase during half-oxidation (by one electron) at the first oxidation peak and then decrease when oxidation (by the second electron) is finished. However, no such bands have been detected for compounds 1–4 in the given experimental conditions (concentration ca. 3 mM, cell thickness 0.2 mm, NIR range 1000–2500 nm). The result thus indicates no or only low electronic communication between the oxidizable substituents in positions 4- and 7- of phenanthroline.

### 2.4. IR Spectroelectrochemistry

The IR spectroelectrochemistry of 1 and 2 does not show significant changes in absorption spectra during the oxidation at the first oxidation wave I. The wide absorption band at  $1633 \text{ cm}^{-1}$ , and other bands at 1577, 1558, 1540, and  $1265 \text{ cm}^{-1}$  corresponding to vibrations of aromatic rings in molecule 1 remained constant. Only a decrease of the absorption bands at

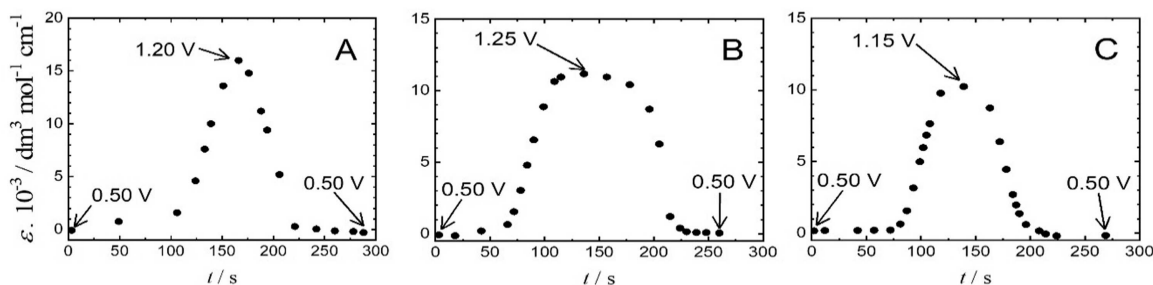


**Figure 5.** Transients of absorption spectra obtained during UV-Vis spectroelectrochemistry of compounds **1** (A), **2** (B) and **3** (C) during oxidation in the first step and the subsequent rereduction.

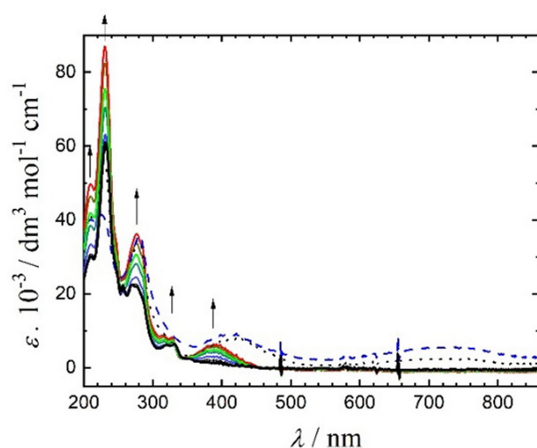


**Figure 6.** UV-Vis spectroelectrochemistry of **4** during oxidation at the first oxidation wave (spectra registered at potentials 0.70, 1.60, 1.64, 1.68, 1.70 and 1.72 V). Dotted and dashed curves show absorption spectrum recorded at 1.75 and 1.78 V, respectively.

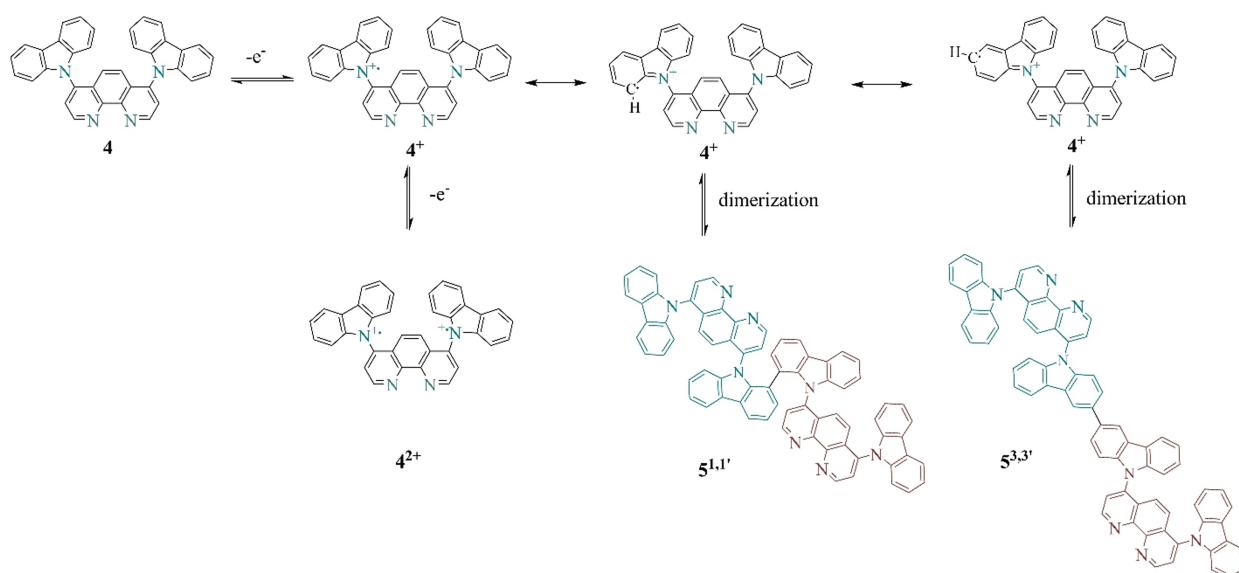
1312 and 1241  $\text{cm}^{-1}$  is observed. The second oxidation process in merged waves II + II' results in the appearance of the characteristic absorption band at 1037  $\text{cm}^{-1}$  corresponding to

the vibration of the S=O functional group (Figure 7A). Simultaneously, the increase of other bands at 1577, 1558, 1519, 1506, 1312, 1284 and 1242  $\text{cm}^{-1}$  is observed.

## 2.5. Identification of Products

Solutions of **2** after electrolysis at potential 1.77 V (i.e. between the II' wave and the III wave) were analysed by HPLC-MS/MS. Both the hypothesized final products 5-methyl-4,7-bis(5-oxido-10H-phenothiazin-10-yl)-1,10-phenanthroline (**2-di(sulfoxide)**, see Scheme 2) and an intermediate species 5-methyl-4-(5-oxido-10H-phenothiazin-10-yl)-7-(10H-phenothiazin-10-yl)-1,10-phenanthroline (**2-sulfoxide**, see Scheme 2) were identified in electrolyzed samples (Figure S9). The characteristic species with retention times, corresponding molecular ions, along with the product ions in tandem mass spectra, are reported in Table 3.

HPLC-MS/MS results did not show any dimer in solution after oxidative electrolysis. This can be due to the instability of dimers in highly oxidized state. This is consistent with the cyclic voltammogram, which does not show the typical response for dimers in multiple scans (Figure S7).



**Scheme 3.** Proposed oxidation mechanism of compound **4** at the oxidation wave I.

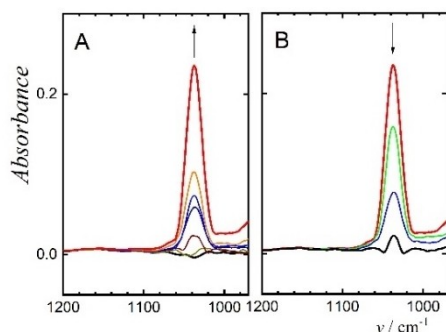


**Figure 7.** IR spectroelectrochemistry of compound **1** A) during oxidation at the waves II + II', B) during backward reduction of product **1-sulfoxide** at 0 V.

Samples of solutions of compounds **2** and **4** taken before and after the exhaustive reductive electrolysis were inspected by HPLC-MS/MS. The identified products were the corresponding species 5-methyl-4-(10*H*-phenothiazin-10-yl)-1,10-phenanthroline (**2-one subst**), 4-(9*H*-carbazol-9-yl)-1,10-phenanthroline (**4-one subst**), which lost one phenothiazine or carbazole substituent from the molecule, and 5-methyl-1,10-phenanthroline and 1,10-phenanthroline formed after the cleavage of both substituents (Figure S10). The characteristic species with retention times, corresponding molecular ions, along with the product ions in tandem mass spectra, are reported in Table 3.

### 3. Conclusions

Investigation of the compounds **1–4** revealed that the substitution on 1,10-phenanthroline by two phenothiazine or two carbazole units leads to the redox system containing two equivalent redox centres, each oxidizable in two subsequent one-electron steps, hence overall by four electrons. Addition of fluorine and methyl groups to the 1,10-phenanthroline of the studied molecules was performed to break the molecule symmetry. Such modification of chemical structure showed the possibility to tune the redox and spectral properties of the phenothiazine phenanthrolines. However, electrochemical and spectroelectrochemical measurements proved low electronic communication between the oxidation centres and consequently the modification (substitution by CH<sub>3</sub> or F) on the

phenanthroline unit bridging the redox centres did not result in a significant change of the oxidation mechanism. Most of the oxidation steps in the studied compound appeared either electrochemically reversible or at least chemically reversible (rereduction in shifted, less positive potentials). We observed a reversible generation of green color (band around 500 nm) due to chromophores attached to 1,10-phenanthroline, compound well-known as excellent bidentate ligand. The intended further study of these compounds will be therefore focused on complexation of various metals with 1,10-phenanthroline core. In particular, the properties of the investigated species can be of advantage to develop sensors containing suitable agents for complexation of metal cations and small organic molecules with the purpose of their detection in wastewater.

### Experimental Section

The experimental part regarding the chromatographic and mass spectrometric analysis is reported in the Supporting Information file.

#### Reagents and Electrochemical Setup

Compounds 4,7-di(phenothiazine)-1,10-phenanthroline **1**, 5-methyl-4,7-di(phenothiazine)-1,10-phenanthroline **2**, 4,7-di(phenothiazine)-5-fluoro-1,10-phenanthroline **3** and 4,7-di(carbazole)-1,10-phenanthroline **4** were synthesized according to the literature.<sup>[22]</sup>

All electrochemical measurements were performed on a PGSTAT 12 Autolab potentiostat (Metrohm, Czech Republic). Cyclic voltammetry was measured in the solution of respective compounds in deaerated 0.1 M tetrabutylammonium hexafluorophosphate (TBAPF<sub>6</sub>, Sigma Aldrich) supporting electrolyte in acetonitrile (anhydrous, water <0.001 %, Sigma Aldrich) in a three-electrode arrangement in a glass cell. The supporting electrolyte was used dried at 90 °C before the use. The Ag|AgCl|1 M LiCl reference electrode was separated from the examined solution by a salt bridge. The glassy carbon working electrode (diameter 0.9 mm) was activated by polishing in Al<sub>2</sub>O<sub>3</sub> aqueous suspension on DP-Nap polishing pad (Struers, Czech Republic). A freshly annealed platinum wire served as the auxiliary electrode. Values of voltammetric faradaic current were obtained by subtracting capacitance current from the total peak current.<sup>[17]</sup> The semi-integration of linear sweep voltammograms (convolution voltammetry) was performed in accordance with literature<sup>[17–18]</sup> and the semi-integrated currents  $I$  were obtained from the equation  $I = \pi^{-1/2} \int_0^t (I(v)/(t-v)^{1/2}) dv$ , where  $v$  is an integration variable and  $t$  is related to the potential through

**Table 3.** Retention time, raw formula, calculated and experimental  $m/z$  for the  $[M+H]^+$  ion and main fragment ions detected in the tandem mass spectra for the solution before and after oxidation for compound **2**, and before and after reduction of both compounds **2** and **4**.

	Compound name	Retention time (min)	Raw formula	Calculated $m/z$ for $[M+H]^+$	Experimental $m/z$ for $[M+H]^+$	$\Delta$ ppm	Fragment ions ( $m/z$ )
<b>2 oxidation</b>	<b>2</b>	24.2	C <sub>37</sub> H <sub>24</sub> N <sub>4</sub> S <sub>2</sub>	589.1521	589.1524	0.5	390.1049
	<b>2-sulfoxide</b>	17.9 and 18.8	C <sub>37</sub> H <sub>24</sub> N <sub>4</sub> OS <sub>2</sub>	605.1470	605.1476	1.0	557.1772, 198.0367
	<b>2- di(sulfoxide)</b>	14.7	C <sub>37</sub> H <sub>24</sub> N <sub>4</sub> O <sub>2</sub> S <sub>2</sub>	621.1419	621.1423	0.6	198.0363
	<b>2 reduction</b>						
<b>2 reduction</b>	<b>2-one subst</b>	18.2	C <sub>25</sub> H <sub>17</sub> N <sub>3</sub> S	392.1221	392.1226	1.3	360.1493, 194.0839
	5-methyl-1,10-phenanthroline	2.0	C <sub>13</sub> H <sub>10</sub> N <sub>2</sub>	195.0922	195.092	−1.0	195.0911, 180.0678, 167.0723
	<b>4</b>	22.8	C <sub>36</sub> H <sub>22</sub> N <sub>4</sub>	511.1923	511.1911	−2.3	465.2232, 319.1908
<b>4 reduction</b>	<b>4-one subst</b>	16.7	C <sub>24</sub> H <sub>15</sub> N <sub>3</sub>	346.1344	346.1357	3.8	331.1101, 180.0686, 166.0647, 153.0574
	1,10-phenanthroline	1.3	C <sub>12</sub> H <sub>8</sub> N <sub>2</sub>	181.0766	181.0768	1.1	154.0655, 127.0546

the scan rate. The logarithmic (log-plot) analysis ( $\log(I/I_{\text{lim}} - I)$  vs.  $E$ ) of semi-integrated currents was obtained according to the procedure described for the steady-state waves in order to obtain the parameters (slope) of the dependence  $E = E_{1/2} + RT/nF \ln(I/I_{\text{lim}} - I)$ .<sup>[17,23]</sup>

The reductive and oxidative exhaustive electrolyses were performed on glassy carbon working electrode in a dedicated glass electrochemical cell containing separated working and auxiliary electrode compartments.

### In-situ Spectroelectrochemical Measurements

The UV-Vis and IR spectroelectrochemistry was performed using an optically transparent thin-layer cell containing the optical windows made of  $\text{CaF}_2$ <sup>[24]</sup> with the platinum net electrode with sufficient optical transparency used as the working electrode. The cell was equipped with Ag/AgCl quasi reference electrode and platinum net auxiliary electrode. All spectroelectrochemical investigations were performed in strictly oxygen-free environment. Absorption spectra in the range 195–1000 nm were measured during the electrolysis in a cyclovoltammetric regime with the scan rate of  $5 \text{ mV} \cdot \text{s}^{-1}$  using an Agilent 8453 diode-array spectrometer. IR spectra in the range of  $4000\text{--}1000 \text{ cm}^{-1}$  and NIR spectra in the range  $10000\text{--}4000 \text{ cm}^{-1}$  were registered using a Nicolet iS50 FTIR spectrometer equipped with KBr and  $\text{CaF}_2$  beam splitters.

### Computational Details

Calculations of frontier molecular orbital spatial distribution and energies were performed using the DFT theory employing the B3LYP functional and 6-31G\* basis set in the environment of Spartan'14, v.1.1.8 software (Wavefunction, Inc. USA). The spatial distribution of HOMO, HOMO(-1) and LUMO orbitals was calculated for the geometry-optimized molecule 1–4 in a vacuum. Values of orbital energies reported further in this work are referenced against vacuum. The calculations of IR spectra were performed in vacuum using the DFT employing the EDF2 functional and 6-31G\* basis set.

### Acknowledgements

Authors kindly acknowledge the project 19-03160S of the Czech Science Foundation and Czech Academy of Sciences (RVO: 61388955). The Visiting Fellows Programme of the University of Pisa is also acknowledged for funding and supporting the collaboration between CAS and the Department of Chemistry and Industrial Chemistry. We thank the Erasmus Plus and "CIS- Chemia i Staze" for the nine months award to stay at J. Heyrovský Institute of Physical Chemistry of the Czech Academy of Sciences in Prague to J. Wantulok.

### Conflict of Interest

The authors declare no conflict of interest.

**Keywords:** 1,10-phenanthroline · electrochemical oxidation and reduction · phenothiazine · breaking molecular symmetry · spectroelectrochemistry

- [1] C. H. Hamann, A. Hammett, W. Vielstich, *Electrochemistry*, Wiley-VCH Verlag GmbH and Co. KGaA, Weinheim, 2007.
- [2] J.-W. Xu, M.-H. Chua, K.-W. Shah, *Electrochromic Smart Materials Fabrication and Applications*, Royal Society of Chemistry, London, 2019.
- [3] a) M. T. Miller, P. K. Gantzel, T. B. Karpishin, *Inorg. Chem.* **1998**, *37*, 2285–2290; b) H. Ferreira, M. M. Conradie, K. G. von Eschwege, J. Conradie, *Polyhedron* **2017**, *122*, 147–154; c) G. L. Smith, Reutovich, A. A. Srivastava, A. K. Reichard, R. E. Welsh, C. H. Melman, F. A. Bou-Abdallah, *J. Inorg. Biochem.* **2021**, *220*, 111460.
- [4] a) K. Itaya, H. Akahoshi, S. Toshima, *J. Electrochem. Soc.* **1982**, *129*, 762–767; b) S. S. Zhang, X. P. Qiu, W. H. Chou, Q. G. Liu, L. L. Yang, B. Q. Xing, *Solid State Ionics* **1992**, *52*, 287–289; c) S. Bernhard, J. I. Goldsmith, K. Takada, H. D. Abruna, *Inorg. Chem.* **2003**, *42*, 4389–4393; d) J. Hwang, J. I. Son, Y. B. Shim, *Sol Energ Mat Sol C* **2010**, *94*, 1286–1292; e) N. Oyama, M. Kitagawa, H. Inaba, K. Kawase, *Macromol. Symp.* **1994**, *80*, 337–351.
- [5] a) J. F. Ambrose, R. F. Nelson, *J. Electrochem. Soc.* **1968**, *115*, 1159–1164; b) W. Lamm, F. Pragst, W. Jugelt, *J. Prakt. Chem.* **1975**, *317*, 995–1004; c) F. Belal, S. M. El-Ashry, I. M. Shehata, M. A. El-Sherbeny, D. T. El-Sherbeny, *Mikrochim. Acta* **2000**, *135*, 147–154; d) K. Mielech-Lukasiewicz, E. Staskowska, *Anal. Sci.* **2015**, *31*, 961–969.
- [6] a) E. T. Seo, R. F. Nelson, J. M. Fritsch, L. S. Marcoux, D. W. Leedy, R. N. Adams, *J. Am. Chem. Soc.* **1966**, *88*, 3498–3503; b) H. Hayen, U. Karst, *Anal. Chem.* **2003**, *75*, 4833–4840; c) B. Blankert, H. Hayen, S. M. van Leeuwen, U. Karst, E. Bodoki, S. Lotrean, R. Sandulescu, N. M. Diez, O. Dominguez, J. Arcos, J. M. Kauffmann, *Electroanalysis* **2005**, *17*, 1501–1510.
- [7] a) N. Prachumrak, S. Pojanasopa, S. Namuangruk, T. Kaewin, S. Jungsuttiwong, T. Sudyoadsuk, V. Promarak, *Acs Appl Mater Inter* **2013**, *5*, 8694–8703; b) J. Y. Li, Q. Li, D. Liu, *Acs Appl Mater Inter* **2011**, *3*, 2099–2107.
- [8] J. L. Li, A. C. Grimsdale, *Chem. Soc. Rev.* **2010**, *39*, 2399–2410.
- [9] a) X. Qian, Y. Z. Zhu, J. Song, X. P. Gao, J. Y. Zheng, *Org. Lett.* **2013**, *15*, 6034–6037; b) G. Marotta, M. A. Reddy, S. P. Singh, A. Islam, L. Y. Han, F. De Angelis, M. Pastore, M. Chandrasekharan, *Acs Appl Mater Inter* **2013**, *5*, 9635–9647; c) A. Venkateswararao, K. R. J. Thomas, C. P. Lee, C. T. Li, K. C. Ho, *Acs Appl Mater Inter* **2014**, *6*, 2528–2539.
- [10] T. Godet-Bar, J. C. Lepretre, O. Le Bacq, J. Y. Sanchez, A. Deronzier, A. Pasturel, *Phys. Chem. Chem. Phys.* **2015**, *17*, 25283–25296.
- [11] a) H. J. Knolker, K. R. Reddy, *Chem. Rev.* **2002**, *102*, 4303–4427; b) A. W. Schmidt, K. R. Reddy, H. J. Knolker, *Chem. Rev.* **2012**, *112*, 3193–3328.
- [12] a) M. J. Ohlow, B. Moosmann, *Drug Discov Today* **2011**, *16*, 119–131; b) E. A. Welker, B. L. Tiley, C. M. Sasaran, M. A. Zuchero, W. S. Tong, M. J. Vettleson, R. A. Richards, J. J. Geruntho, S. Stoll, J. P. Wolbach, I. J. Rhile, *J. Org. Chem.* **2015**, *80*, 8705–8712; c) F. F. Yong, A. M. Mak, W. Q. Wu, M. B. Sullivan, E. G. Robins, C. W. Johannes, H. Jong, Y. H. Lim, *ChemPlusChem* **2017**, *82*, 750–757; d) M. Garcia-Iglesias, K. Peuntinger, A. Kahnt, J. Krausmann, P. Vazquez, D. Gonzalez-Rodriguez, D. M. Guld, T. Torres, *J. Am. Chem. Soc.* **2013**, *135*, 19311–19318.
- [13] a) J. I. Ahamed, M. F. Valan, K. Pandurengan, P. Agastian, B. Venkatadri, M. R. Rameshkumar, K. Narendran, *Res Chem Intermediat* **2021**, *47*, 759–794; b) B. Morak-Mlodawska, K. Pluta, K. Suwinska, M. Jelen, *J. Mol. Struct.* **2017**, *1133*, 398–404.
- [14] X. C. Pan, C. Fang, M. Fantin, N. Malhotra, W. Y. So, L. A. Peteanu, A. A. Isse, A. Gennaro, P. Liu, K. Matyjaszewski, *J. Am. Chem. Soc.* **2016**, *138*, 2411–2425.
- [15] M. Baete, T. Gessner, H.-W. Schmidt, M. Thelakkat, Phenothiazines, S-oxides, and S,S-dioxides as well as phenoxazines as emitters for OLEDs. Patent n. US8029919B2, Current Assignee UDC Ireland Ltd. **2010**, pp. 31–32.
- [16] J. Wantulok, R. Sokolova, I. Degano, V. Kolivoska, J. E. Nycz, *Electrochim. Acta* **2021**, *370*, 137674.
- [17] A. J. Bard, L. F. Faulkner, *Electrochemical Methods: Fundamentals and Applications - 2nd ed.*, John Wiley & Sons, New York, 2001.
- [18] a) J. C. Imbeaux, J. M. Saveant, *J. Electroanal. Chem.* **1973**, *44*, 169–187; b) T. Pajkossy, *Electrochem. Commun.* **2018**, *90*, 69–72.
- [19] a) J. B. Flanagan, S. Margel, A. J. Bard, F. C. Anson, *J. Am. Chem. Soc.* **1978**, *100*, 4248–4253; b) F. Ammar, J. M. Saveant, *J. Electroanal. Chem.* **1973**, *47*, 215–221; c) N. Das, A. M. Arif, P. J. Stang, M. Sieger, B. Sarkar, W. Kaim, J. Fiedler, *Inorg. Chem.* **2005**, *44*, 5798–5804.
- [20] J.-M. Savéant, *Elements of Molecular and Biomolecular Electrochemistry. An Electrochemical Approach to Electron Transfer Chemistry*, John Wiley and Sons, Inc., New Jersey, 2006.



- [21] a) K. Y. Chiu, T. X. Su, J. H. Li, T. H. Lin, G. S. Liou, S. H. Cheng, *J. Electroanal. Chem.* **2005**, 575, 95–101; b) L. Kortekaas, F. Lancia, J. D. Steen, W. R. Browne, *J. Phys. Chem. C* **2017**, 121, 14688–14702.
- [22] a) J. E. Nycz, J. Wantulok, R. Sokolova, L. Pajchel, M. Stankevic, M. Szala, J. G. Malecki, D. Swoboda, *Molecules* **2019**, 24; b) G. Zucchi, V. Murugesan, D. Tondelier, D. Aldakov, T. Jeon, F. Yang, P. Thuery, M. Ephritikhine, B. Geffroy, *Inorg. Chem.* **2011**, 50, 4851–4856.
- [23] J. Heyrovsky, J. Kuta, *Principles of Polarography*, Publishing House of the Czechoslovak Academy, Prague, **1965**.
- [24] M. Krejčík, M. Danek, F. Hartl, *J. Electroanal. Chem.* **1991**, 317, 179–187.

Manuscript received: June 19, 2021

Revised manuscript received: July 9, 2021

Accepted manuscript online: July 19, 2021